



## Field observations of wave-driven water-level gradients across a coral reef flat

O. K. Jago,<sup>1</sup> P. S. Kench,<sup>1</sup> and R. W. Brander<sup>2</sup>

Received 1 June 2006; revised 5 March 2007; accepted 19 March 2007; published 30 June 2007.

[1] Field measurements of still water surface elevations were obtained across a narrow leeward reef flat on Lady Elliot Island, Great Barrier Reef, Australia in June 2003. Stilling wells were deployed from the reef crest landward to the island beach, and waves and mean water levels were monitored over both rising and falling tides during low to moderate wave energy conditions. Wave setup of up to 13.8 cm above still water level occurred in the presence of incident waves of 0.4 m yielding maximum water surface slopes greater than  $6^\circ$ . Results show that the magnitude of wave setup varies both temporally and spatially across the reef with changing water depth. Setup is dominant on the reef edge at low tide, evolving into a dual setup system at both the reef edge and shoreline at midtide and finally a dominant shoreline setup at high tide. On Lady Elliot Island the dual setup system is considered to result from spatial differences in transformation and breaking of swell and wind waves at midtide stages. The presence of a dual setup system across a reef flat has not been previously identified in field or modeling studies and has potentially significant implications for reefal current development, sediment transport, and the stability of reef island shorelines.

**Citation:** Jago, O. K., P. S. Kench, and R. W. Brander (2007), Field observations of wave-driven water-level gradients across a coral reef flat, *J. Geophys. Res.*, 112, C06027, doi:10.1029/2006JC003740.

### 1. Introduction

[2] Coral reefs represent the interface between deep ocean waves and associated reef landforms, and their physical structure creates a hydrodynamic environment markedly different from continental beach systems that have been the primary focus of nearshore hydrodynamic research. The coral reef hydrodynamic environment is fundamentally determined by the steep transition from relatively deep to shallow water across which ocean waves propagate. Furthermore, the presence of calcareous organisms forming the reef surface provides a substantially rougher boundary surface than that experienced on a sandy continental shoreline [Massel and Brinkman, 1999; Zhu *et al.*, 2004]. The interaction of wave processes and the reef surface is of increasing interest for modeling wave energy fluxes that have been shown to affect factors such as reef organism distribution [Chappel, 1980; Geister, 1977; Roberts *et al.*, 1992; Storr, 1964; Storlazzi *et al.*, 2005], geomorphic development of reef systems [Munk and Sargent, 1948; Roberts, 1974; Roberts *et al.*, 1992; Kench, 1998a; Engels *et al.*, 2004; Kench and McLean, 2004; Storlazzi *et al.*, 2003], and island shoreline stability [Brander *et al.*, 2004;

Gourlay, 1988, 1990; Hopley, 1981; Kench and Brander, 2006].

[3] To date, the majority of hydrodynamic reef studies have focused primarily or solely on the distinct transition zone between the fore reef and the outer reef flat [Lee and Black, 1978; Lugo-Fernández *et al.*, 1994, 1998a, 1998b; Massel and Brinkman, 1999; Nelson and Lesleighter, 1986; Roberts *et al.*, 1977; Roberts and Suhayda, 1983; Tsukayama and Nakaza, 2001]. These studies have noted dramatic reductions in wave energy associated with wave breaking from offshore to backreef environments ranging from 58 to 97% depending on individual reef morphology and water depth at the reef crest. In contrast, there are few studies of wave processes on reef flats behind this zone. While the formation and character of reformed waves have been relatively well described [Gourlay, 1994, 1996; Hardy *et al.*, 1990; Lugo-Fernández *et al.*, 1994; Massel, 1996; Nelson, 1994], subsequent propagation and transformation of such waves across reef flats is largely unknown [Brander *et al.*, 2004; Kench and Brander, 2006].

[4] Transformations in wave energy, both at the reef edge and across the reef flat, will have important effects on water-level gradients across the reef surface. Wave setup at the reef edge has been identified in a number of studies [Tait, 1972; Jensen, 1991; Gourlay, 1993] and has been explained using the concept of radiation stress [Longuet-Higgins and Stewart, 1964] whereby energy loss due to wave breaking and frictional damping in the surf zone generates a cross-reef gradient in radiation stress ( $S_{xx}$ ) which is balanced by an offshore pressure gradient analogous to the plane beach solution outlined by Longuet-Higgins and Stewart [1964]

<sup>1</sup>School of Geography, Geology and Environmental Science, The University of Auckland, Auckland, New Zealand.

<sup>2</sup>School of Biological, Earth and Environmental Sciences, University of New South Wales, Sydney, Australia.

and *Bowen et al.* [1968]. The net result is the minimum mean water level at the wave breakpoint, while the maximum water level will occur at the landward extent of swash processes [*Bowen et al.*, 1968].

[5] Understanding wave setup in low-lying reef environments is important as water-level gradients resulting from wave transformations are able to drive mean currents and circulation within reef systems [*Hearn et al.*, 2001; *Kraines et al.*, 1999, 2001; *Massel and Brinkman*, 1999, 2001; *Munk and Sargent*, 1948; *Symonds et al.*, 1995]. Consequently, setup-driven flows are of geomorphic significance as they determine the transport of sediment around reef systems and islands, and also control the flow and exchange of oceanic water throughout reef systems, that subsequently determines reef productivity [*Kraines et al.*, 1998; *Stoddart*, 1969].

[6] Although the significance of wave setup in reef systems has been recognized, there have been few studies of this phenomenon. Studies which have examined wave setup have adopted modeling approaches, including numerical [*Gourlay and Colleter*, 2005; *Hearn*, 1999; *Kraines et al.*, 1998; *Symonds et al.*, 1995; *Tait*, 1972] and physical laboratory models [*Gourlay*, 1993, 1996, 1997; *Jensen*, 1991]. These studies have identified two primary patterns of wave setup and associated cross-reef flat water-level patterns; the exact form of which is determined by gross reef structure and its relationship to landforms. First, in fringing reef settings (backed by a shoreline), maximum water level is thought to occur landward of the reef edge, where wave-breaking ceases, and it is assumed that water level remains constant across the reef flat as there are no further transformations in wave energy [*Gourlay*, 1993, 1994, 1996; *Massel and Brinkman*, 1999; *Tait*, 1972]. In this model the shoreline provides a barrier to the flow produced by the hydraulic gradient across the reef flat [*Young*, 1989], and *Gourlay* [1996] identified the potential for further wave setup to occur as reformed oscillatory waves finally break on the beach. Second, in barrier reef systems, an open backreef water body allows the pressure gradient across the reef surface to be redressed [*Gourlay and Colleter*, 2005; *Hearn et al.*, 2001]. This generates a sloping water surface from a maximum at the point of cessation of wave breaking to the mean water level in the backreef [*Gourlay*, 1996; *Hearn et al.*, 2001]. The magnitude of wave setup has been shown to be dependent on wave height [*Gourlay*, 1996, 1997; *Hearn*, 1999; *Symonds et al.*, 1995; *Tait*, 1972], being on the order of 10 to 20% of incident wave height [*Hopley*, 1982; *Massel and Brinkman*, 2001]. Furthermore, it has been demonstrated that water depth over the reef surface moderates wave setup whereby setup is maximized at low water depths and ceases where depth is sufficient to allow the propagation of waves without breaking [*Gourlay*, 1993; *Hearn*, 1999; *Symonds et al.*, 1995; *Tait*, 1972].

[7] However, these modeling approaches have involved a number of simplifications. First, studies have focused almost exclusively on a two-dimensional (cross reef) approach. Second, models have been developed on oversimplified reef morphologies with constant fore reef slopes and horizontal reef flat surfaces, and common topographic features such as coral colonies, rubble ridges, paleoreef surfaces, and algal ridges have been neglected. In one exception, *Gourlay and Colleter* [2005] attempted to account for surface roughness

on reef systems. These features have been noted to cause wave transformations through shoaling, further breaking, and bottom frictional damping [*Brander et al.*, 2004; *Jago*, 2005] and may therefore influence water-level gradients across the reef surface. Furthermore, it is difficult to assess the accuracy of proposed setup models as, to date, there have been few attempts to measure wave-induced water-level gradients across entire extents of reef flats. *Kench* [1998b] measured broad-scale water-level differences of 15 to 20 cm between the windward and leeward reefs of the Cocos (Keeling Islands), while *Munk and Sargent* [1948] estimated differences of approximately 45 cm between offshore and reef surface water levels. At a smaller scale, *Lugo-Fernández et al.* [1998b] measured water-level differences of 0.8 to 1.5 cm between the reef crest and backreef at Tague Reef, St Croix. This study describes detailed field measurements of the magnitude of still water levels across the full extent of a reef flat from the reef crest to the reef island shoreline. The aim is to examine temporal and spatial variations in wave setup across the reef flat.

## 2. Study Location

[8] The study was conducted on Lady Elliot Island (24°07'S, 152°43'E) located 83 km off the east coast of Queensland, Australia in the southern limit of the Great Barrier Reef (Figure 1). The Lady Elliot Reef platform is mid-Holocene in age and is approximately 1400 m wide and long covering an area of 1.9 km<sup>2</sup> [*Flood et al.*, 1979; *Chivas et al.*, 1986]. The reef platform supports a vegetated island 0.54 km<sup>2</sup> in area with an average elevation of 4.5 m above mean sea level (MSL) [*Hopley*, 1982], composed of near-concentric shingle ridges of carbonate material bound by phosphatic cement that have been developing at a nearly uniform rate for approximately 3200 years [*Chivas et al.*, 1986]. Beaches on the leeward side of Lady Elliot Island demonstrate clear cusp and berm development, both of which are visibly active throughout the tidal cycle and are indicative of significant wave and swash action.

[9] Reef flat morphology varies considerably from windward to leeward sides of the island. The windward (eastern) reef flat is approximately 360 m wide with a mean elevation of 0.8 m below MSL on the inner reef and 0.2 m below MSL on the outer reef platform where an algal ridge has developed (Figures 1c and 1d). In contrast, the leeward reef flat is narrow (50–60 m) and lower in elevation (1.0 m below MSL, Figure 1c and 1e).

[10] The leeward reef flat can be divided into two broad ecomorphological zones. First, the outer reef flat extends approximately 15 to 20 m shoreward from the reef crest and is variable in elevation being dominated by thickets of branching coral (*Acropora* sp.) separated by deeper channels. Second, the inner reef flat is relatively constant in elevation and supports minimal growth of live coral, with the reef substrate covered by coarse sediments consisting of coral, mollusks, and foraminifera.

[11] The hydrodynamic conditions at the southern extremity of the Great Barrier Reef are poorly documented. The tidal regime at Lady Elliot Island is marked by semidiurnal mesotides with a strong diurnal inequality [*Hopley*, 1982]. Spring and neap tide ranges are 1.7 and 0.9 m, respectively. Southeasterly trade winds prevail for 70% of the year

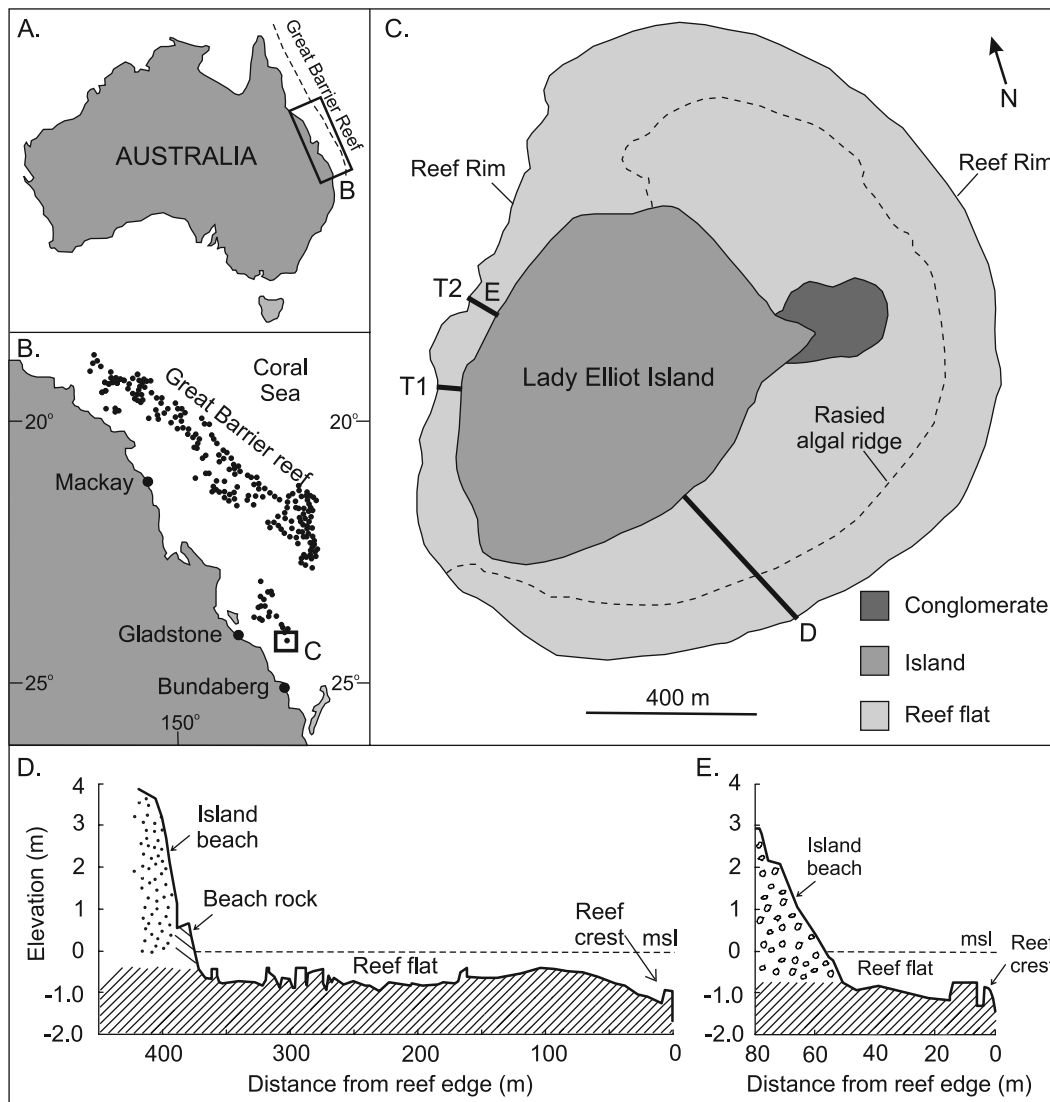


**Figure 1.** (a, b) Location and (c) reef platform configuration of Lady Elliot Island, southern Great Barrier Reef, Queensland, Australia. (d, e) Differences in reef flat topography on the windward and leeward side of the island. Location of stilling well experiments across leeward reef platform are indicated (T1 and T2).

[Flood, 1977]. However, during winter months, winds tend to demonstrate a greater southerly component [Hopley, 1982]. Annual mean wind speed recorded at Lady Elliot Island is approximately  $20 \text{ km h}^{-1}$ . Flood [1977] estimated that swell waves 1 to 3 m in height dominate the Lady Elliot wave climate. On the basis of the closest wave data from the Gold Coast, Australia, Hopley [1982] reported that significant wave height exceeds 1.15 m 50% of the time and only for 0.01% of the time exceeds 4.0 m.

### 3. Methods

[12] Detailed temporal and spatial measurements of water surface elevation were made across the leeward reef flat of Lady Elliot Island in June 2003 using nine slow-response stilling wells (SW) similar to those used in previous surf zone studies [Nielsen, 1999; Nielsen et al., 2001; Haas et al., 2002; Baird et al., 2004]. The stilling wells were made

of 2-m-long clear acrylic tubes (internal diameter of 44 mm) and were attached to steel poles inserted into the reef surface. Water entered each well through the bottom which was packed with tightly rolled 90- $\mu\text{m}$  filter cloth extending 40 mm from the base. The purpose of this approach was for the water level inside the tube to equilibrate to the mean water level outside the tube while filtering out high-frequency gravity wave energy. To test this approach and to establish the response time of water level inside the wells, pressure sensors (KPSI Series 550 Water Level Monitors) were used to generate a synchronous high-frequency water-level record from within and outside the tube. A pressure sensor was placed in the base of each stilling well with a second sensor attached to the exterior of the tube. Both sensors were mounted at the same elevation and were programmed to sample continuously at 2 Hz for 1 h. Consequently, the external sensor measured the full spectrum of wave frequencies, whereas the internal sensor

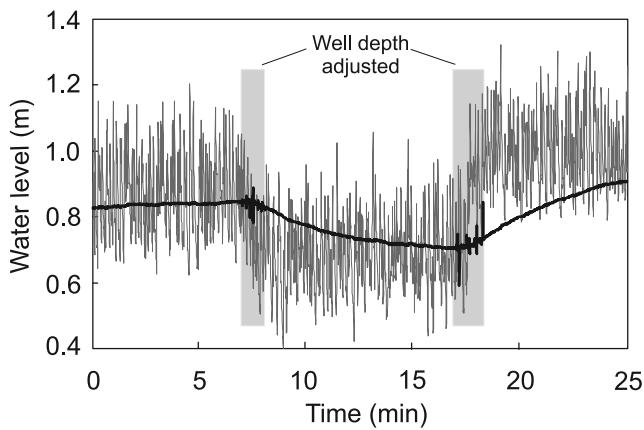


**Figure 2.** Comparison of high-frequency water-level records outside (grey line) and inside (black line) a stilling well. Note waves up to 0.45 m outside well compared with smooth water-level record inside well. Vertical light gray bars are periods when the well was adjusted in elevation.

measured the filtered water level. Furthermore, the water depth around the stilling well was changed every 10 min (by up to 0.25 m) by physically adjusting stilling well elevation to allow detection of the response time of water level within wells.

[13] Results showed that wells filtered all energy in gravity wave frequencies, and no longer period oscillations were observed in the stilling well water-level record (Figure 2). The response time of water level inside the SW (i.e., time lag for water level to respond to changes in external mean water level) ranged from 4.2 to 4.4 min. This response time is beyond the influence of shorter-period infragravity wave frequencies (30 to 240 s). Consequently, test data indicates that water level inside the well was not responsive to water-level oscillations at either the gravity or higher infragravity wave frequencies.

[14] Before each experiment commenced, fluorescent dye was added to each stilling well to aid in the differentiation between the water level in the well and the surrounding reef flat. The elevation of still water level below the top of the tube was read from an externally mounted metric tape. Measurements were manually read to the nearest millimeter with a repeatable error of  $\pm 1$  mm. Measurements were made at 3-min intervals with one person responsible for two wells. Because of the time interval between the measurements of adjacent wells (less than 30 s), the time of each measurement was recorded using synchronized stop watches. Following data collection, a time series of water level in each well was constructed and water levels at each 3-min interval extracted from each continuous time series.

[15] To reduce water levels to a common datum, a total station was used to survey the top of each stilling well to a temporary benchmark before the commencement of each

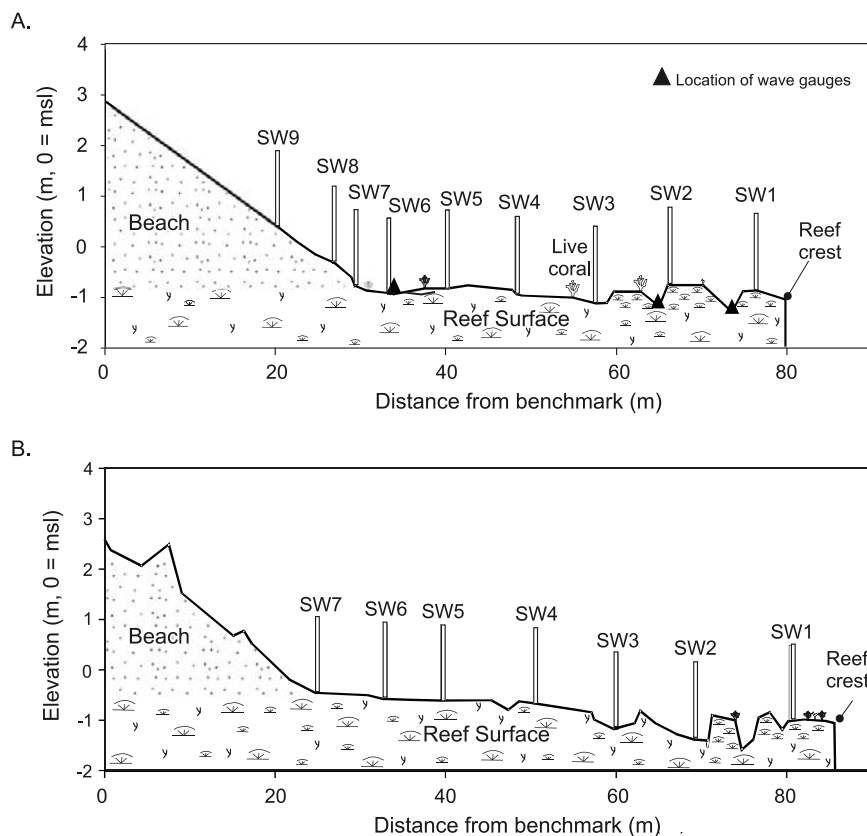


**Figure 3.** Reef flat topography at stilling well experiment sites (a) T1 and (b) T2. Position of stilling wells and wave gauges indicated. Note difference in inner reef flat elevation between transects. Location of reef transects on the reef platform is indicated in Figure 1c.

**Table 1.** Summary of the Four Stilling Well Measurement Periods Conducted Across the Leeward Reef Flat, Lady Elliot Island<sup>a</sup>

	Experiment 1	Experiment 2	Experiment 3	Experiment 4
Date	28 June 2003	28 June 2003	30 June 2003	1 July 2003
Time	9:30–11:09	14:18–17:18	14:57–17:12	12:36–13:45
Profile Location	T1	T1	T2	T2
Tidal Stage	Midlate falling	Midlate rising	Early rising	Late falling
No. Wells Measured	7	9	7	6

<sup>a</sup>The number of wells measured represents the maximum number of wells monitored during each experiment.

experiment. This allowed mean water levels in each well to be calculated with respect to the temporary benchmark and enabled the comparison of water levels across the reef transect. Because of tidal influence, the mean water level across all active wells along the profile was averaged, and data were presented as the difference between the mean water surface (MWS) for the profile and the water level measured at each stilling well. For ease of presentation, cross-reef variations in water level were time stacked and presented as contour plots.

[16] Measurements were conducted along two transects with differing morphology on the leeward reef flat (T1 and T2, Figure 3) separated by a longshore distance of approximately 200 m. Along each transect, two measurement periods were conducted to encompass periods of rising and falling tides (Table 1). At each site, stilling wells were positioned in a two-dimensional cross-shore array, stretching from the reef edge to the shoreline, and were numbered sequentially from the reef edge landward (Figure 3).

[17] The reef flat along T1 (Figure 3a) was characterized by relatively uniform topography with a mean elevation approximately 0.8 m below mean sea level (MSL). Maximum elevation (0.6 m below MSL) was on the outer reef flat, close to the reef edge, where dense live branching coral growth dominated. The reef flat along T2 (Figure 3b) had a slightly higher mean elevation (approximately 0.6 m below MSL). However, maximum elevation along this transect occurs in the inner reef flat (0.5 m below MSL) and is 0.3 m higher in elevation at the beach/reef interface than T1 (Figure 3b). There was also a notable lack of live coral growth over the landward half of the inner reef flat of T2. The elevation of the inner reef flat is approximately equal to the upper limit of live coral growth on T1, suggesting that the elevation of the reef flat in relation to tidal elevation precludes coral growth in this region.

[18] In addition to stilling well data, wave characteristics were measured along each transect on the outer reef flat surface (<5 m from the reef crest), middle reef flat (20 m from the reef crest), and on the toe of beach (Figure 3a). Waves were measured using a Doble wave gauge on the outer reef flat and two InterOcean S4 current meters with on board pressure sensors. The instruments were programmed to sample at 2 Hz for 17.1 min every half hour. Wave data was analyzed to examine cross-reef flat wave characteristics at different tidal stages and transformations in wave energy. Estimates of significant wave height ( $H_s$ ) were obtained using the standard deviation of the pressure sensor records ( $H_s = 4\sigma$ ), and significant wave period was estimated through zero-downcrossing analysis. Spectral analysis was performed using Matlab on bursts of 2048 samples to

determine the peak energy and the variance associated with different gravity and infragravity frequencies. All spectra were analyzed with 16  $df$  with a high-frequency cutoff value of 1 Hz.

## 4. Results

### 4.1. Wave and Water-Level Conditions

[19] Incident wave energy recorded at the reef edge was moderate to low, with  $H_s$  remaining below 0.43 m throughout the measurement period (Figure 4). Values of  $H_s$  ranged from 0.43 m at higher-tidal stages to 0.05 m at lower-tidal stages. Although wave height is clearly modulated by tidal stage (water depth), it is not purely dependent on water depth. This is particularly true during high-tide periods when the wave height is small relative to water depth and wave breaking is reduced. At such tidal stages, waves are able to pass over the reef crest without breaking so that waves are representative of the offshore wave conditions. Overall, wave period ( $T_s$ ) decreased from 8–11 s during the first half of the deployment to 3–8 s in the second half (Figure 4c). Longer wave periods are associated with low-tide conditions.

### 4.2. Wave Transformations Across the Reef Flat

[20] Results of the analysis of wave gauges deployed across the reef flat surface also indicate that the propagation of wave energy toward the beach is influenced by water depth. Results showed remarkable consistency in the degree of wave energy transformation across the reef surface at different stages of the tide with a summary example of results presented in Figure 5. At high-tide stages the wave height (maximum of 0.43 m) to water depth ratio indicates that waves are in intermediate water depths, have not broken at the reef crest, and are likely be shoaling. This accounts for the marginal increase in  $H_s$  values between the outer and central reef flat (Figures 5a and 5b). Spectral analysis of the high-tide wave records indicates two important features of wave characteristics on the reef flat (Figure 5d). First is that wave energy is grouped around two prominent frequency bands, swell wave energy (0.11 Hz, 9 s), which is dominant, and wind wave energy (0.25 Hz, 4 s). Second is that, as waves shoal across the reef flat, reduction in energy is low relative to previous studies of wave energy transformation. While energy in the wind wave frequency exhibits little change between instrument stations, energy in the swell wave frequency is reduced by 50% between the reef crest and the toe of beach (Figure 5d).

[21] At middle tide stages, water depth limitations at the reef crest induce breaking of higher waves with continued dissipation of bores across the reef flat. This accounts for

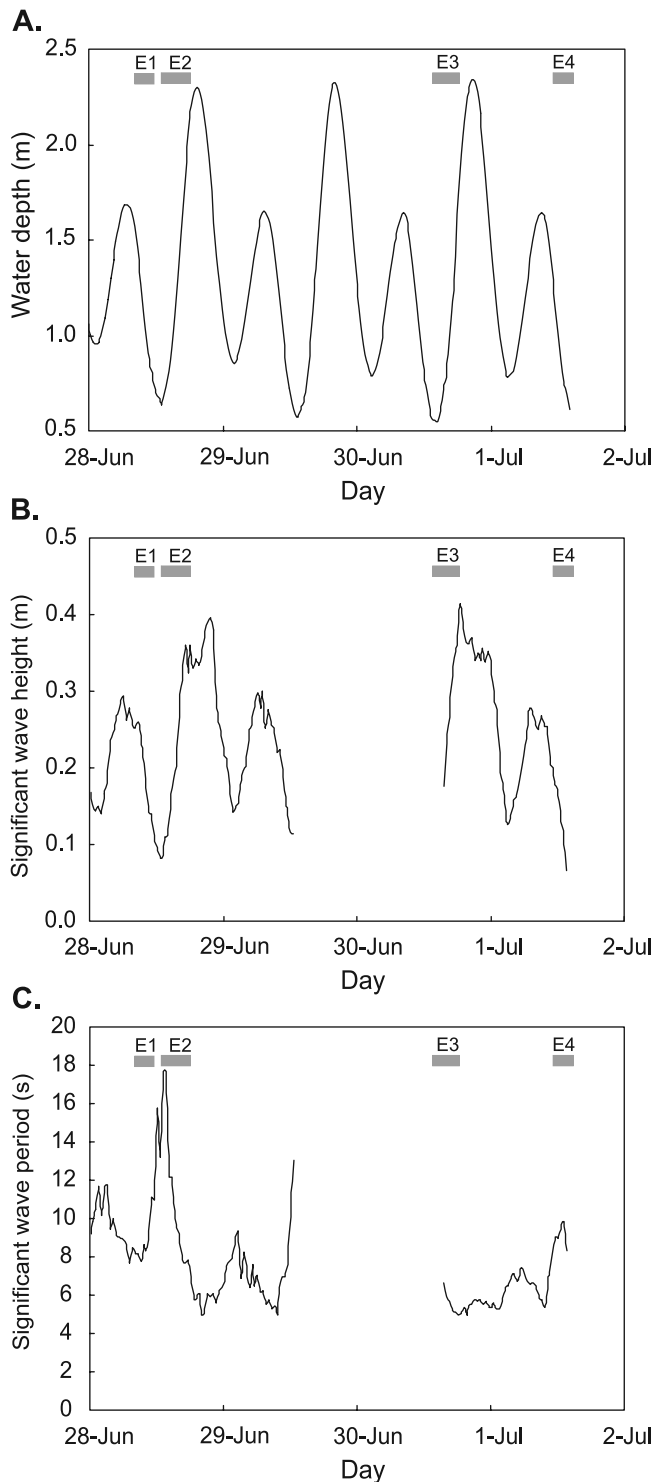


**Figure 4.** Conditions measured at the leeward reef crest throughout the period of stilling well experiments on transect T1 depicting the following: (a) water depth  $h$ , (b) significant wave height  $H_s$ ; and (c) significant wave period  $T_s$ . E1–E4 identify the period of stilling well experiments.

the decrease in  $H_s$  toward the beach (Figures 5e, 5f, and 5g). Comparison of spectra at this time (Figure 5h) shows that wind wave energy has decreased in prominence at all locations (compared to high tide, Figure 5d) reflecting the

breaking of these larger waves on the reef crest. The spectra also show that there is a relatively small attenuation of swell energy (22%) across the reef flat. Consequently, wave processes across the reef flat are similar to a surf zone with larger, shorter period, waves breaking on the outer reef flat and dissipation of bores across the reef, but smaller swell waves continuing to shoal and break across the reef flat.

[22] At lower-tidal stages, water depth limitations act to filter both wind and swell wave energy from the reef flat surface as demonstrated by the reduced  $H_s$  values at each location (Figures 5i, 5j, 5k, and 5l). Under these water level conditions, wave energy is more effectively attenuated across the reef flat (by 98% at the swell and wind wave frequencies, Figure 5l). Therefore the reef flat wave conditions resemble an inner surf zone dominated by bores, which dissipate the remaining energy across the reef flat.

[23] In summary, at higher-tidal stages, there is relatively little change in wave energy across the reef flat surface. In contrast, at lower water levels, most gravity wave energy is attenuated between the outer reef flat and toe of beach. Note that, at all tidal stages, there is growth in energy in the infragravity wave frequency across the reef flat. However, spectra indicate that this energy is very small, and raw data suggest that infragravity motions at around 64 s (0.02 Hz, Figures 5d, 5h, and 5l) have wave amplitudes up to 0.035 m (Figure 5k).

### 4.3. Water-Level Gradients

[24] Figures 6 and 7 show time stacks of water-level differences across the reef flat at T1 and T2, respectively, for the four measurement periods and encompass both falling and rising tide conditions at each location. Water levels are reported relative to the MWS, and for the purposes of this analysis, positive elevations are considered to represent regions of wave setup. Each measurement period is now described.

#### 4.3.1. T1, Falling Tide

[25] The falling tide during the first measurement period at T1 was characterized by a decrease in water depth from 1.39 to 0.85 m (0.55-m range) and a corresponding decrease in  $H_s$  from 0.25 to 0.14 m (Figure 3). Variations in cross-reef flat water levels during this time show several spatial and temporal trends (Figure 6a). Maximum water levels across the reef flat were consistently restricted to the following two regions: (1) the reef flat just landward of the reef edge (SW2), and (2) the shoreline (SW7). Similarly, regions of lower water levels were also consistent in location, occurring at (1) the outer reef flat (SW1) and at (2) the central reef flat (SW5). Setup was highest on the outer reef flat reaching a maximum of 2.7 cm above MWS ( $\bar{X} = 1.8$  cm) and tended to increase with the falling tide (Figure 6a). The lowest water levels occurred at the reef crest and increased from  $-0.05$  to  $-4.1$  cm below MWS as more wave shoaling and breaking took place immediately landward of this zone as the tide fell. Subsequently, maximum water-level differences across the reef (7.6 cm) occurred between SW2 and SW1 resulting in a seaward water surface gradient of  $0.42^\circ$ . This region also coincided with the most variable and rapidly changing topography of the reef profile (Figure 6a), and the highest topographic point on the reef surface coincided with the highest relative water level.

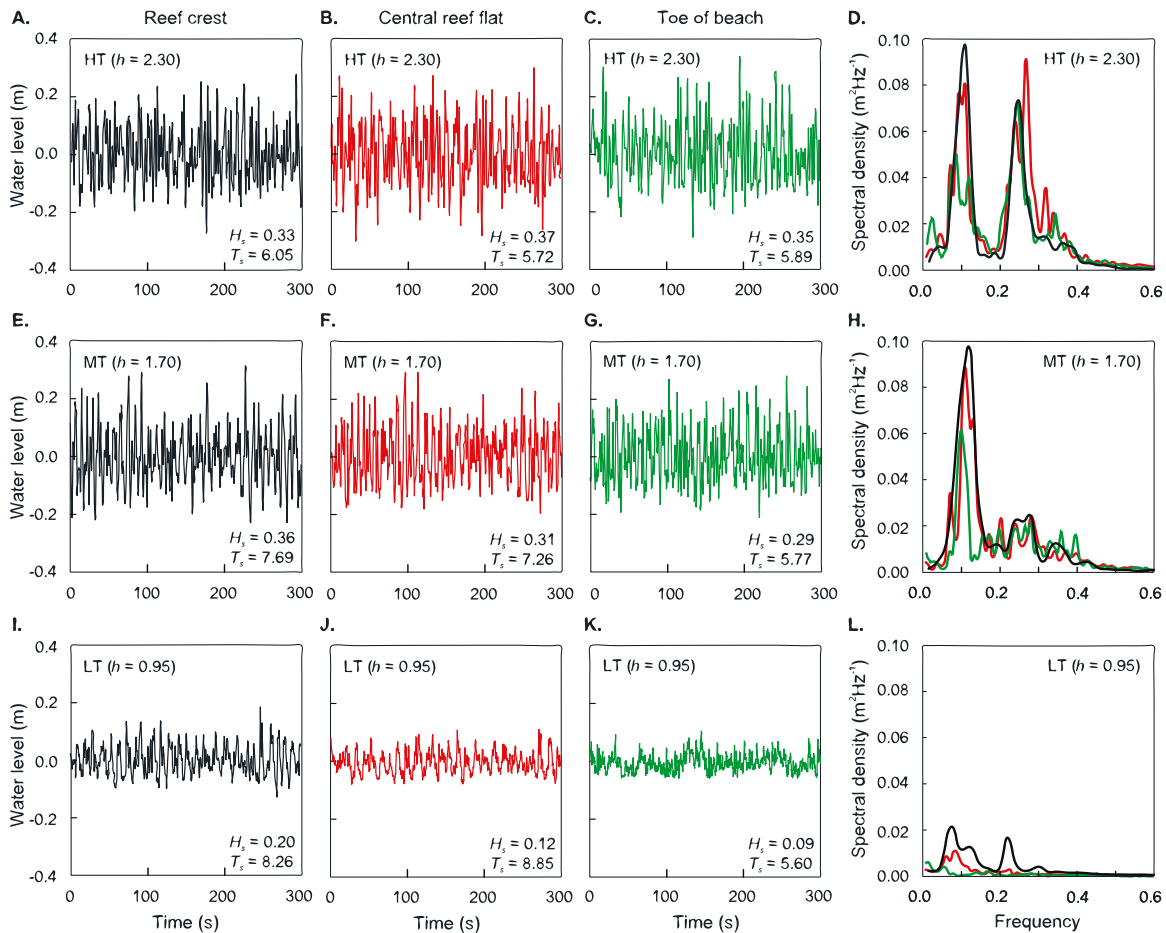


**Figure 5.** Cross-reef flat differences in wave characteristics at different tidal stages on transect T1, 28 June 2003. Short (300 s) wave records are presented for the reef crest, central reef flat, and toe of beach at (a, b, and c) high tide, (e, f, and g) midtide, and (i, j, and k) lower tidal stage. Spectral plots (Figures 5d, 5h, and 5l) highlight wave energy and frequency differences across the reef flat at different tidal stages. Note,  $H_s$  and  $T_s$  values are based on the longer 2048 point data sets. Water depth ( $h$ ) at each tidal stage is the water depth at the reef crest. Location of instruments shown on Figure 3.

[26] A smaller, positive water-level gradient existed between SW5 and SW2 (Figure 6a) associated with a gradual increase in relative water level with decreasing tidal stage. The two most shoreward stilling wells measured water levels at, or slightly above, MWS (up to 0.7 cm), with SW7 recording consistently higher values than SW6 (Figure 6a). These inner wells exhibited little variation in relative water level throughout the experiment (Figure 6a). Similarly, the planar and featureless central reef flat region was also characterized by minimal cross-shore change in water surface elevation.

#### 4.3.2. T1, Rising Tide

[27] The rising tide during the second measurement period at T1 was characterized by an increase in water depth from 0.74 to 1.91 m (1.17-m range) and a corresponding increase in  $H_s$  from 0.11 to 0.33 m (Figure 4). An additional two stilling wells were deployed landward of SW 7 on the beachface (Figure 6b). Initially, regions of low water level occurred at the reef edge ( $-3$  cm) and at the central reef flat between SW3 and SW4 (1 to  $-2$  cm), whereas setup was restricted to the reef edge between SW1 and SW2 ( $+1$  cm) and seaward of the shoreline between SW5 and SW7 ( $+1$  to

4 cm; Figure 6b). These patterns changed markedly during the rising tide. First, setup was primarily restricted to the shoreline increasing to a maximum of 10.7 cm at high tide (SW9, Figure 6b). Second, the maximum difference between stilling wells (13.8 cm) occurred between SW9 (maximum) and SW3 (minimum). At this time the maximum seaward-directed water slope was  $1.65^\circ$  between stilling wells 9 and 8.

[28] Third, the point of minimum water level migrated landward. SW2 represented the lowest point of mean water surface elevation on the reef platform after 36 min of sampling ( $-3.0$  cm, Figure 6b), and there was no apparent primary setup system at the reef edge. Setup only occurred at the landward limit of wave propagation, most likely associated with the cessation of wave breaking at the reef edge due to increased water depth and transfer of the breaker zone close to the shoreline (Figures 5a, 5b, 5c, and 5d).

[29] Fourth, relative water level at SW1 continued to increase rising above the mean level of the reef platform after 69 min of sampling ( $+1.0$  cm). The gradient between SW1 and SW2 peaks at  $0.18^\circ$  (landward) or a difference of 3.3 cm 129 min after initial measurements. Consequently,

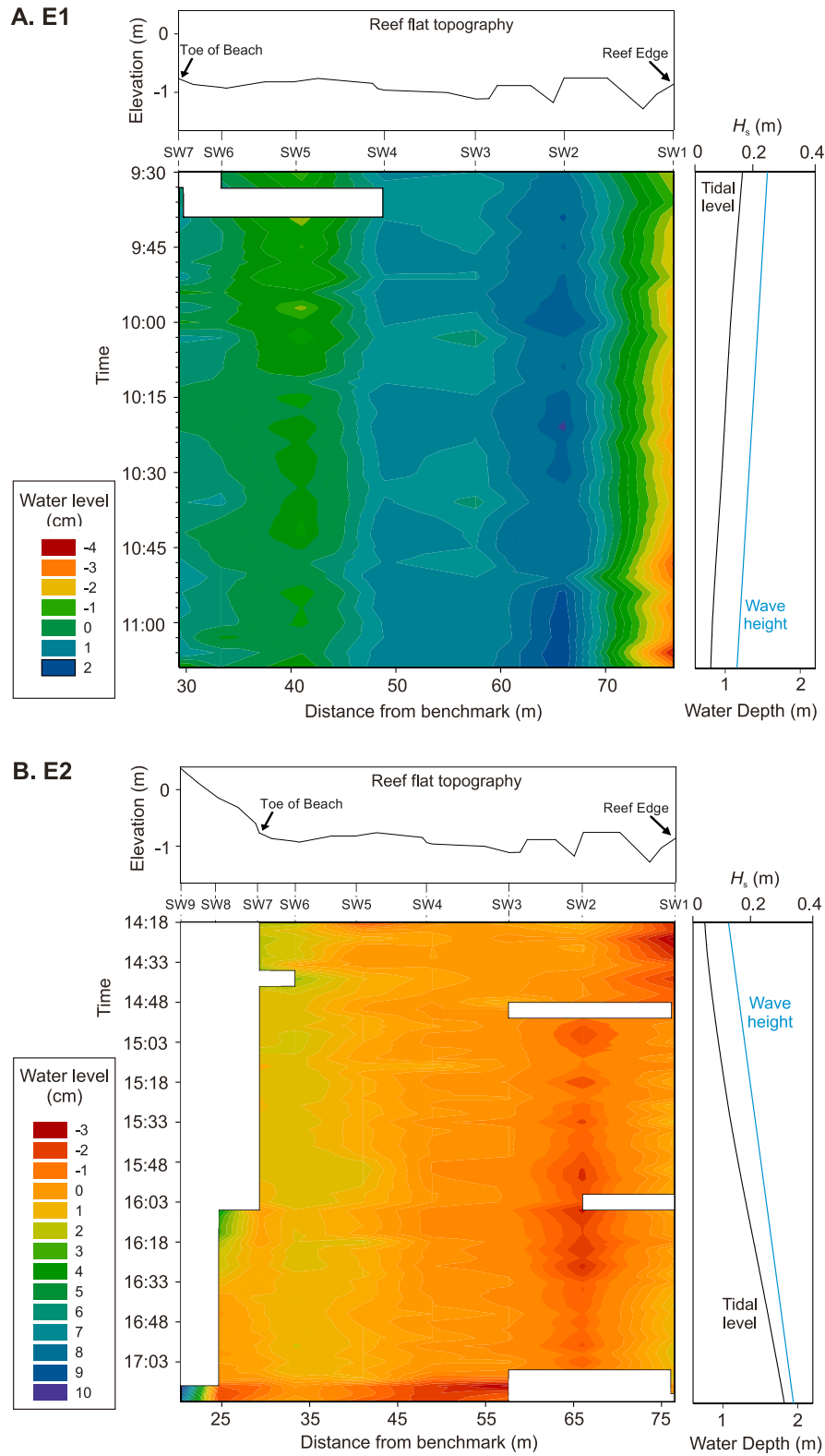


**Figure 6.** Summary results of reef flat water levels measured on the (a) falling tide and (b) rising tide at transect 1 (T1). Both Figures 6a and 6b present the reef profile showing stilling well locations, change in tidal level and  $H_s$  measured at the reef crest, and time-stacked water level measurements across the reef profile (color contour plot). Water level measurements were recorded at 3-min intervals.

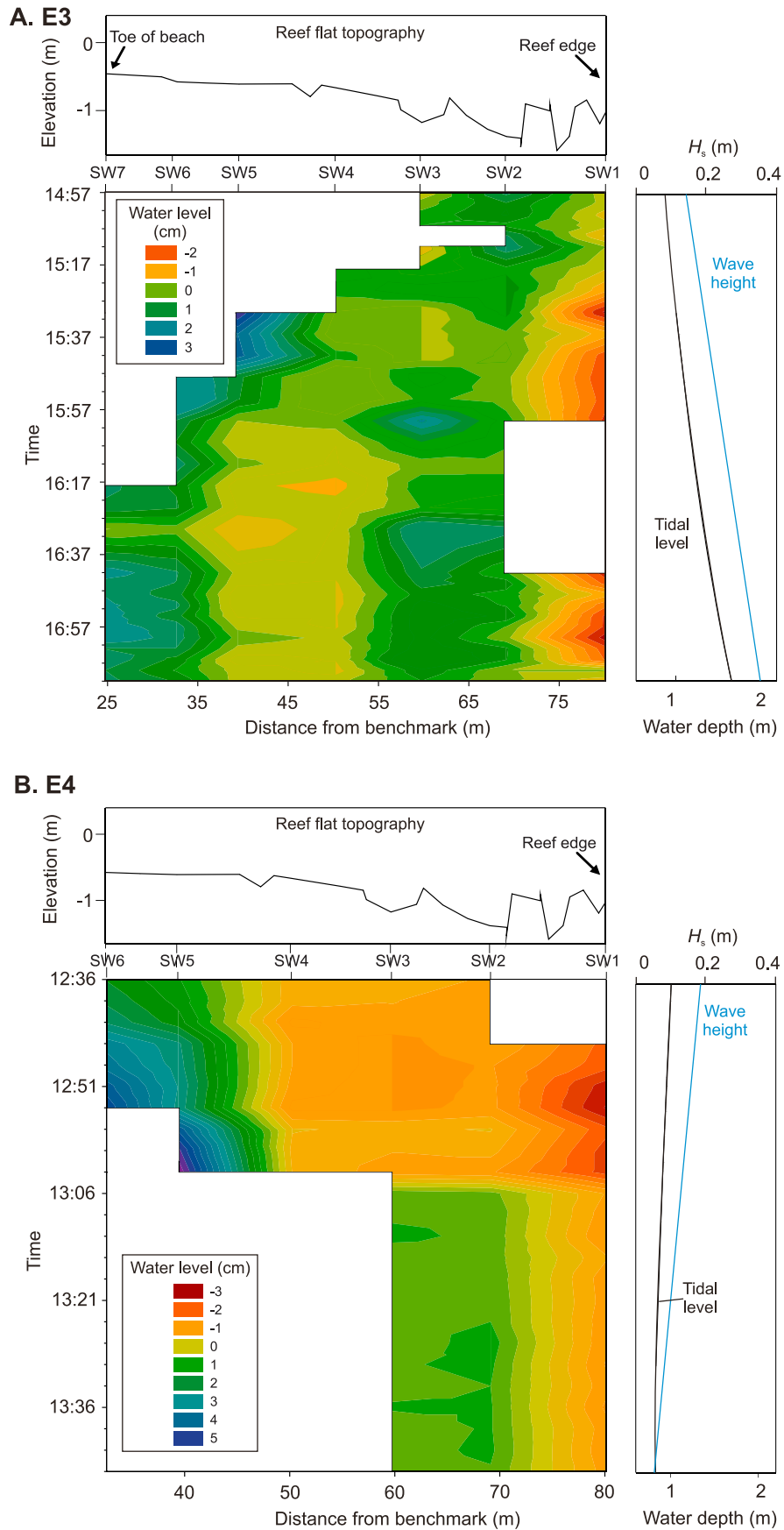
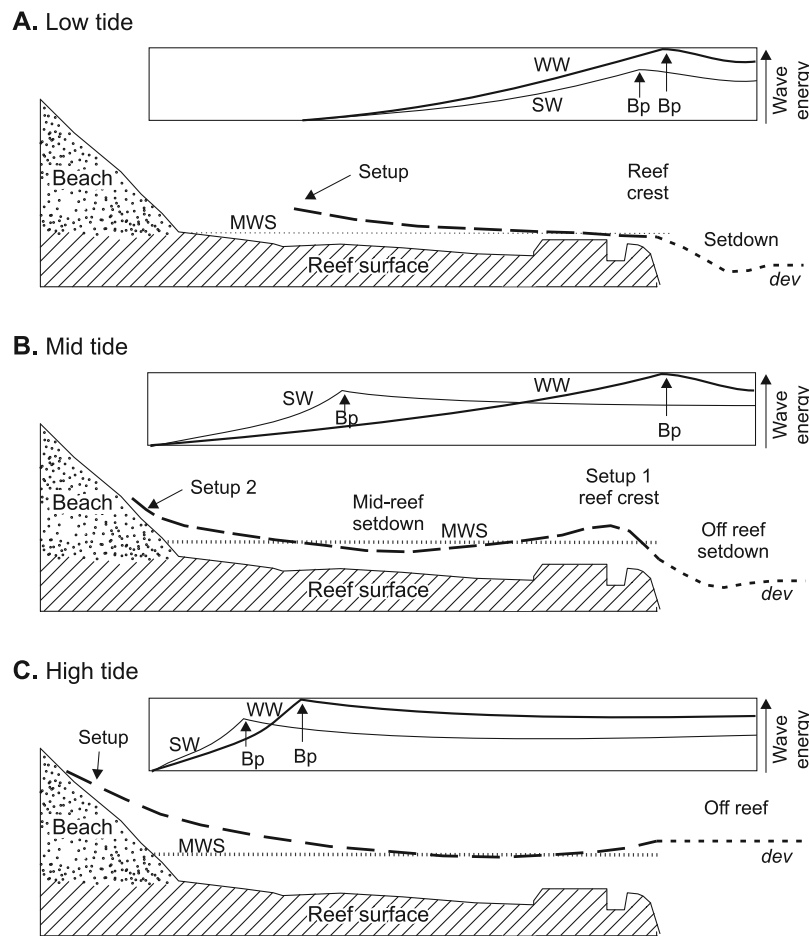


Figure 7



**Figure 8.** Schematic representation of wave setup and setdown across a reef flat at different tidal stages. Dashed lines represent profiles of the deviation of water level (dev) from the mean water surface (MWS) in the presence of waves at the following: (a) low tide, (b) midtide, and (c) high. The dotted line seaward of the reef edge indicates the expected water surface deviation offshore of the reef crest. Note that differences in water surface elevation across the reef platform have been vertically exaggerated. Inset panels in Figures 8a, 8b, and 8c represent the growth of wave energy due to shoaling of wind waves (WW) and swell waves (SW) to the breakpoint (Bp) and subsequent energy decay through the surf zone.

there is an increasing landward-directed water gradient at the reef edge as water depth increases.

[30] During this sampling period, the highest water level was consistently measured at the most landward active stilling well (Figure 6b). Furthermore, the magnitude of this maximum can be seen to increase with the slope of the bed over which the swash processes were operating (Figure 6b). Initially, maximum water elevation at the landward extent of wave processes was +2.0 cm (SW7). As water depth increased to inundate SW8 and SW9, which represents the transition from the reef flat to the progressively steeper toe of beach and upper beach, the elevation of the MWS increased to 3.6 and 10.7 cm at SW8 and SW9, respectively.

[31] In general, a landward migration of the major water level zones is evident accompanying the rise in tide level

(Figure 6b). The zone of minimum water level translated from SW1 shoreward to SW2, while the zone of maximum water level migrated landward as the increasing water depth allowed wave and swash processes to operate further across the stilling well transect.

#### 4.3.3. T2, Rising Tide

[32] During the rising tide measurement period at T2, water depth increased from 0.55 to 1.42 m (0.87-m range) and  $H_s$  increased from 0.15 to 0.35 m (Figures 4 and 7a). This experiment was characterized by two areas of higher water level with maximum setup at the shoreline and at SW3. These two areas were separated by a zone of lower water on the central reef flat (SW4). A second zone of lower relative water level occurred at the reef edge (SW1) and

**Figure 7.** Summary results of reef flat water levels measured on the (a) falling tide and (b) rising tide at transect 2 (T2). Both Figures 7a and 7b present the reef profile showing stilling well locations, change in tidal level and  $H_s$  measured at the reef crest, and time-stacked water level measurements across the reef profile (color contour plot). Water level measurements were recorded at 3-min intervals.

persisted through most of the rising tide before diminishing close to higher-tidal stages (Figure 5a).

[33] Patterns of water surface elevation during the rising tide show that maximum elevation is largely restricted to the limit of wave excursion on the reef flat (Figure 7A). The highest elevation above MWS was 3.3 cm, recorded in the initial measurement at SW5, which created a water level difference of 6.1 cm between SW1 and SW5. Results also show a rapid decrease in relative water elevation at shoreward locations as water depth increased and the maximum extent of swash and wave processes translated shoreward. For example, water level at SW5 declined from 3.3 to 0.8 cm above MWS within 18 min, and after 30 min, water level fell below MWS (Figure 7a) representing a depression between the higher water-level zones.

[34] The second region of relatively high water level at SW3 is pronounced during the second half of the rising tide (Figure 7a). At this location, water level peaked at 1.8 cm above MWS, creating a 4.2-cm difference, or a  $0.18^\circ$  seaward-directed gradient in the water surface to SW1. Differences between SW3 and SW2 are generally small throughout this period (<1 cm). However, initially, water level at SW2 was higher than that at SW3 by up to 2.2 cm. Relative water level at SW3 became increasingly positive during the rising tide, while SW2 experienced a transition to slightly negative values (Figure 7a).

[35] Relative water level at the reef edge (SW1) became increasingly negative through the rising tide until the last half hour of measurements (Figure 7a). This location represented the lowest water surface elevation in each measurement, reaching a minimum of 2.8 cm below MWS and up to 4.5 cm below the highest point measured on the transect. Direct comparison with SW2 reveals that the gradient of the water surface over the outer reef increased over the duration of the experiment, largely attributable to the relative decrease in water elevation measured at SW1. It is interesting to note that this is a reversal of the trend noted during the falling tide, most likely associated with the reversal in water depth changes over the sampling period.

#### 4.3.4. T2, Falling Tide

[36] The falling tide during the experiment at T2 was characterized by a decrease in water depth from 1.01 to 0.61 m (0.4-m range) and a corresponding decrease in  $H_s$  from 0.18 to 0.06 m (Figures 4 and 7b). There was a consistent increase in relative water level across the reef platform, with maximum setup at the shoreline (Figure 7b). The maximum seaward-directed water gradient was  $0.33^\circ$  between SW4 and SW5 at the commencement of measurement at SW5. The maximum difference in water elevation between SW1 and SW6 reached 7.6 cm and is of similar magnitude to the 8.1-cm difference between SW1 and SW5 measured at the final sample of SW5 (Figure 7b).

[37] Maximum still water elevation occurred closest to the landward extent of wave runup. Initially, water elevation reached a maximum at SW6 located at the shoreline (+4 cm, Figure 7b). However, as water level fell, the position of highest water level migrated across the reef controlled by the limit of wave processes (swash). It is also evident that the magnitude of the raised water level increases as water depth over the reef flat decreases. This is likely to be the

result of stilling wells providing a better approximation of the limit of wave runup as water depth over the reef platform decreases. For example, the water surface elevation at SW6 was 1.6 cm above MWS at the start of the experiment and reached a maximum of 4.6 cm as the tide fell and when the maximum extent of swash penetration retreated toward SW6.

[38] Throughout this period, there is very little difference in the relative elevation of the still water surface on the central reef flat (SW2-SW4, Figure 7b). However, at the reef edge, there is a large difference between SW1 and SW2, indicating a second water surface gradient. The water surface at SW1 remained below MWS throughout the experiment, attaining a maximum of 3.0 cm below MWS (Figure 7b). The gradient between these sites reduced with decreasing water depth.

## 5. Discussion

[39] Results represent the first detailed measurements of water-level gradients across a reef flat extending from the outer reef flat to island shoreline, in the presence of gravity wave energy, and demonstrate that detectable differences in mean water level of up to 13.8 cm exist across relatively narrow (60 m) reef flats. Such water level differences cannot be accounted for by the offshore sea breezes ( $<5 \text{ ms}^{-1}$ ) that prevailed during experiments or the presence of standing infragravity motion. Infragravity motion is shown to be negligible at high-tidal stages (Figure 5d). Energy at infragravity frequencies is shown to increase toward lower-tidal stages (Figure 5l); however, peak wave heights of 0.05 m are well below the maximum water-level variations observed and have a period (around 64 s) that is dampened by the stilling wells (Figure 2). Consequently, water-level differences are believed to be attributed to the presence and transformation of incident wave energy across the reef flat.

[40] Here we examine the magnitude and temporal and spatial variability in observed wave setup gradients across the reef platform. A number of setup systems are identified, associated with changes in water depth that control the spatial distribution of shoaling, breaking, and postbreaking wave transformations across the reef flat. Implications for reef platform circulation, sediment transport processes, and modeling of wave setup on coral reefs are highlighted.

### 5.1. Magnitude of Setup

[41] The results of this study generally conform to theoretical predictions for wave setup in beach environments. The highest mean water elevations were consistently measured at the landward extent of wave runup, in agreement with the observations of *Bowen et al.* [1968] and *Gourlay* [1992], and the magnitude of wave setup appeared to be related to the gradient of the substrate, as previously noted by *Bowen et al.* [1968] and *Gourlay* [1992]. Sampling at the T1 shoreline revealed a maximum difference between consecutive stilling wells of 10.5 cm, which incorporated the steep beach (gradient of  $6.98^\circ$ ), whereas the maximum difference at the T2 shoreline was 4.5 cm measured across the lower gradient ( $0.28^\circ$ ) inner reef surface. This suggests that considerably more wave energy is lost rapidly with the final turbulent wave breaking over steeper gradients (at T1) than the gradual loss of energy over lower-gradient reef

surfaces (at T2). However, because of limited samples at T1 and limited variations in substrate gradient at this site, this relationship requires further verification. Maximum values of setup ranged from 25 to 40% of the outer reef flat  $H_s$  or 25% of the incident  $H_s$  (as recorded in the outer reef flat wave gauge at high-tide conditions, Figure 4).

[42] The majority of the studies incorporating wave setup in reef environments have focused solely on the fore reef to outer reef flat [Gerritsen, 1981; Gourlay, 1990, 1996; Hearn, 1999; Massel and Gourlay, 2000; Seelig, 1983; Symonds et al., 1995; Tait, 1972; Tartinville and Rancher, 2000]. It is not possible to compare the magnitude of wave setup with these predominantly model-based studies, as no offshore water level was measured to compare water surfaces at the reef edge and over the reef platform. Furthermore, the models incorporate over generalized (flat) reef surfaces with monochromatic wave inputs. However, the magnitude of water-level differences measured in this study exceed the 0.8- to 1.5-cm differences measured by Lugo-Fernández et al. [1998b] over a barrier reef system. This discrepancy can most likely be attributed to the differing morphologies of the reef systems studied and the spatial scales of measurement employed. The open backreef lagoon present in the study site of Lugo-Fernández et al. [1998b] provided a means of redressing the pressure gradient created over the reef surface that may not be present at Lady Elliot Island. Furthermore, Lugo-Fernández et al. [1998b] employed only two measurement points, with the second located in the backreef lagoon, and maximum setup is likely underestimated as the water surface elevation tends toward the offshore value in the lagoon.

## 5.2. Patterns of Setup

[43] Results demonstrate that wave setup variations across the reef platform are associated with changes in tidal stage and relative water depth, which control wave-breaking processes across the reef flat. Three different conditions of setup that represent an evolution of wave setup patterns throughout the tidal cycle are recognized (Figure 8). A single-wave setup system is apparent at low-tidal stages (Figure 8a) with water elevations increasing gradually from a minimum at the reef crest landward across the reef flat. The steepest water-level gradient and highest water surface elevation occur at the maximum extent of wave processes on the inner reef flat. This pattern of water surface elevation was most clearly illustrated by the measurements during the late falling tide at T2 (Figure 7a). Wave conditions on the reef flat that control water-level gradients are characteristic of an inner surf zone. At lower-tidal stages the reef crest acts as an effective filter to incident wave energy (Figures 5i, 5j, 5k, and 5l). Waves break on the reef crest and outer reef flat, and bores continue to be dissipated across the central reef surface.

[44] In contrast to low-tide stages, two wave setup systems occur on the reef flat at midtides (Figure 8b). This represents a distinct departure from wave setup models previously proposed [Gourlay, 1996; Massel and Brinkman, 1999; Symonds et al., 1995; Tait, 1972]. The first setup system occurs over the reef crest and outer reef flat region and is particularly evident during the sampling periods conducted during the midfalling tide at T1 (Figure 6a) and the rising tide at T2 (Figure 7b).

[45] A zone of relative water depression is evident at the reef crest, indicating that maximum wave height is reached at this point. Following this, dissipation of wave energy over the outer reef flat leads to a zone of relatively high water immediately landward of the reef crest. This region of setup generally conforms to patterns established through modeling studies where maximum water surface elevation is attained a short distance from the reef crest at the cessation of breaking processes [Gourlay, 1994, 1996; Lugo-Fernández et al., 2004; Massel and Brinkman, 1999, 2001; Massel and Gourlay, 2000].

[46] A second zone of wave setup occurs at the landward extent of the reef flat, or the island beach (Figure 8b), and results from the final dissipation of reformed waves across the reef flat and transformation of swell wave energy. Such a secondary setup system has not been previously incorporated within existing wave setup models. Gourlay [1996] and Gourlay and Colleter [2005] did acknowledge the possibility of additional shoreline setup, but presented this setup operating on top of a uniformly raised water level created at the reef crest, rather than as an independent system distinguished from the reef edge by a zone of lower water in the central reef flat region, as the findings of this study illustrate (Figures 6 and 8b).

[47] Analysis of cross-reef flat wave characteristics at midtide stages (Figures 5e, 5f, 5g, and 5h) also suggests that wave transformation processes and the interaction of different wave types may be responsible for the observed dual setup system. High-tide spectra indicate that the incident wavefield is dominated by waves at swell (0.11 Hz) and wind wave frequencies (0.25 Hz, Figure 5d). Midtide spectra show that wind wave energy is significantly reduced on the outer reef surface (Figure 5h) indicating that these higher- and shorter-period waves have undergone turbulent breaking at the reef crest and is likely responsible for the setup system at the reef crest. Postbreaking bores continue to be dissipated across the reef flat. In contrast, swell wave energy propagates onto the reef flat without breaking (Figure 5h), then shoals and breaks across the central to inner reef flat promoting setup at the shoreline. Consequently, the dual setup system observed on Lady Elliot Island is probably the result of the presence of a bimodal wave spectrum, with the discrete wave frequencies interacting and transforming differently with the reef at midtidal stages. This contrasts with modeling studies that typically assume a monochromatic wavefield.

[48] Previous studies have assumed that the mean water level can only be returned to the open ocean level through connection to an open body of water, commonly a backreef lagoon. Such a lagoon does not exist at Lady Elliot Island nor in many fringing reef settings. Observations indicate that water levels return to the still water level (or below) on the reef flat surface. Of significance is what mechanism allows the still water surface to be returned to the open ocean level (or lower) on the midreef surface. A likely explanation in this study is alongshore variations in the magnitude of wave setup, which drive along-reef current flows. This could be generated at the study site by differences in reef elevation apparent between the two experimental transects (Figure 3). Jago [2005] measured substantial along-reef flows on the Lady Elliot Island reef flat. As waves propagate across the reef surface, there is

insufficient forcing to maintain the elevated sea surface, and mean flows to areas of lower wave setup may act to redress any pressure gradients existing in an along-reef direction. Subsequently, the elevation of the water surface over the central region of the reef flat is reduced. Consequently, along-reef flows may perform the same function as cross-reef flows through a connection to the open ocean in modeling studies. The implementation of a two-dimensional approach in modeling studies precludes the consideration of alongshore flows as an avenue to redress pressure gradients created at the reef edge. However, the results of this study suggest that it may be of significance in determining the water elevation upon which the secondary setup system will be superimposed and that along-reef variations in setup may be critical in controlling reef top current patterns.

[49] The final pattern of wave setup over the reef flat (Figure 8c) occurs when water depth is sufficient to allow propagation of measured swell and wind waves across the reef crest without breaking or causing significant loss of energy (Figures 5a, 5b, 5c, and 5d, 8c). Waves shoal and increase in height over the outer reef flat and the minimum water elevation is shifted landward from the reef edge (Figure 8c). Landward of this point, minor energy losses due to bottom friction create a gradual increase in the water surface elevation. Finally, wave energy is expended through breaking on the island beach, creating a substantial water-level gradient landward of the beach toe. As there is no setup at the reef crest (Figure 8c), this setup system at the island shoreline is the primary wave setup system, as opposed to the secondary system identified at midtide (Figure 8b). The focus of previous research on waves that break at the reef crest has generally excluded the possibility of the primary setup system occurring at the island beach.

### 5.3. Geomorphic Implications

[50] Recognition of spatial and temporal variations in wave setup across reef platforms have significant implications for reef top circulation and geomorphic processes. Alongshore variations in setup, promoted by variations in reef and beach topography, are likely to drive and control patterns of reefal currents and also provide the mechanisms for balancing wave setup gradients on coral reef platforms and also control reef sedimentation. Setup-driven currents are likely to control sediment transport gradients on reef surfaces and, in part, determine sediment transfer and depositional nodes on reef platforms. Furthermore, the magnitude of shoreline setup will enhance wave runup processes that control the upper limit of deposition contributing to building of the marginal ridges of reef islands. Such controls have previously not been identified in investigations of reef sediment transport processes.

## 6. Conclusions

[51] In contrast to previous modeling approaches, field measurements at Lady Elliot Island, Great Barrier Reef indicate that wave setup varies spatially and temporally across reef flats. In the case of a relatively narrow, leeward reef platform under moderate wave energy conditions on Lady Elliot Island, wave setup zones can occur simultaneously across the platform at the following: (1) the reef crest, as commonly identified in modeling studies and

(2) the swash limit on the inner reef flat or island beach. This second region of setup has received little attention in previous attempts to model setup mechanisms on reefs. Significantly, the two setup zones are separated by a region of lower water level over the central reef flat.

[52] Temporal variations in setup are modulated by tidal stage and associated changing water depths across the reef that control the location of wave shoaling, breaking, and surf zone processes across the reef flat. Setup is dominant on the reef edge at low tide, evolving into a dual setup system at both the reef edge and shoreline at midtide and finally a dominant shoreline setup at high tide. Note that measurements in this study were undertaken under low to moderate wave energy conditions. The incident wavefield was characterized by a bimodal wave spectrum with prominent energy peaks at swell and wind wave frequencies. The differences in interaction of these discrete wave types with the reef at different tidal stages is considered responsible for the observed dual setup system. Under conditions of higher wave energy, it is probable that initial wave breaking will take place on the outer reef under all tidal conditions so that a dual setup system is likely to prevail at middle- to high-tide stages.

[53] While results provide broad agreement with previous modeling studies, detailed cross-reef measurements highlight significant departures from existing model considerations. In particular, the presence of multiple setup systems across a reef surface and the potential for generation of setup-driven currents that balance setup and control reef top circulation, sediment flux, and flushing. These observations should provide insights into refining future two-dimensional models of cross-reef wave setup and developing three-dimensional considerations of wave-driven circulation on reef platforms.

## References

- Baird, M. E., M. Roughan, R. W. Brander, J. H. Middleton, and G. J. Nippard (2004), Mass transfer limited nitrate uptake on a coral reef flat, Warraber Island, Torres Strait, Australia, *Coral Reefs*, 23, 386–396.
- Bowen, A. J., D. L. Inman, and V. P. Simmons (1968), Wave set-down and set-up, *J. Geophys. Res.*, 73, 2569–2577.
- Brander, R. W., P. S. Kench, and D. Hart (2004), Spatial and temporal variations in wave characteristics across a reef platform, Warraber Island, Torres Strait, Australia, *Mar. Geol.*, 207, 169–184.
- Chappell, J. (1980), Coral morphology, diversity and reef growth, *Nature*, 286, 249–252.
- Chivas, A. S., J. Chappell, H. Polach, B. Pillans, and P. Flood (1986), Radiocarbon evidence for the timing and rate of island development, beach-rock formation and phosphatization at Lady Elliot Island, Queensland, Australia, *Mar. Geol.*, 69, 273–287.
- Engels, M. S., C. H. Fletcher III, M. E. Field, C. D. Storlazzi, E. E. Grossman, J. J. B. Rooney, C. L. Conger, and C. Glenn (2004), Holocene reef accretion: Southwest Molokai, Hawaii, U.S.A., *J. Sediment Res.*, 74(2), 255–269.
- Flood, P. G. (1977), The three southernmost reefs of the Great Barrier Reef Province—an illustration of the sequential/evolutionary nature of reef type development, in *1977 Field Conference, Lady Elliot Island- Fraser Island- Gayndah- Biggenden*, edited by R. W. Day, pp. 37–48, Geol. Soc. Aust. Queensland Division, Brisbane.
- Flood, P. G., S. Harjanto, and G. R. Orme (1979), Carbon-14 dates, Lady Elliot Reef, Great Barrier Reef, *Qld. Gov. Min. J.*, 80, 444–447.
- Geister, J. (1977), The influence of wave exposure on the ecological zonation of Caribbean coral reefs, in *Proc. 3rd Int. Coral Reef Symp.*, pp. 23–29, Miami.
- Gerritsen, F. (1981), Wave attenuation and wave set-up on a coastal reef, in *Proc. 17th Int. Conf. Coast. Eng.*, pp. 444–459, ASCE.
- Gourlay, M. R. (1988), “Coral Cays” products of wave action and geological processes in a biogenic environment, in *Proc. 6th Int. Coral Reef Symp.*, pp. 491–496, Townsville.

- Gourlay, M. (1990), Waves, set-up and currents on reefs, cay formation and stability, in *Proceedings of the Engineering in Coral Reef Regions Conference*, pp. 249–264, Townsville.
- Gourlay, M. R. (1992), Wave set-up, wave run-up, and beach water table: Interaction between surf zone hydraulics and groundwater hydraulics, *Coastal Eng.*, *17*, 93–144.
- Gourlay, M. R. (1993), Wave set-up and wave-generated currents on coral reefs, in 11th Australasian Conference on Coastal and Ocean Engineering, pp. 479–484.
- Gourlay, M. R. (1994), Wave transformation on a coral reef, *Coastal Eng.*, *23*, 17–42.
- Gourlay, M. R. (1996), Wave set-up on coral reefs: 1. Set-up and wave-generated flow on an idealized two dimensional horizontal reef, *Coastal Eng.*, *27*, 161–193.
- Gourlay, M. R. (1997), Wave set-up on coral reefs: some practical applications, in Combined Australian Coastal Engineering and Ports Conference, pp. 959–964.
- Gourlay, M. R., and G. Colleter (2005), Wave-generated flow on coral reefs—An analysis for two-dimensional horizontal reef-tops with steep faces, *Coastal Eng.*, *52*, 353–387.
- Haas, K. A., I. A. Svendsen, R. W. Brander, and P. Nielsen (2002), Modeling of a rip current system on Moreton Island, Australia, in Proc. 28th Int. Conf. Coastal Eng., pp. 784–796, ASCE, Cardiff.
- Hardy, T. A., I. R. Young, R. C. Nelson, and M. R. Gourlay (1990), Wave attenuation on an offshore coral reef, in Proceedings of the 22nd International Conference on Coastal Engineering, pp. 330–344, Delft.
- Hearn, C. J. (1999), Wave-breaking hydrodynamics within coral reef systems and the effect of changing relative sea level, *J. Geophys. Res.*, *104*(C12), 30,007–30,019.
- Hearn, C. J., M. J. Atkinson, and J. L. Falter (2001), A physical derivation of nutrient-uptake rates in coral reefs: Effects of roughness and waves, *Coral Reefs*, *20*, 347–356.
- Hopley, D. (1981), Sediment movement around a coral cay, Great Barrier Reef, Australia, *Pac. Geol.*, *15*, 17–36.
- Hopley, D. (1982), *Geomorphology of the Great Barrier Reef: Quaternary Development of Coral Reefs*, 453 p., Wiley-Interscience, Hoboken, N. J.
- Jago, O. K. (2005), Hydrodynamic processes on a coral reef platform: Lady Elliot Island, Great Barrier Reef, M. thesis, 304 pp., Univ. of Auckland.
- Jensen, O. J. (1991), Waves on Coral Reefs, in *Symposium on Coastal and Ocean Management, Coastal Zone '91: Proceedings of the Sixth Symposium on Coastal and Ocean Management*, pp. 2668–2680.
- Kench, P. S. (1998a), Physical controls on development of lagoon sand deposits and lagoon infilling in an Indian Ocean atoll, *J. Coastal Res.*, *14*, 1014–1024.
- Kench, P. S. (1998b), Physical processes in an Indian Ocean atoll, *Coral Reefs*, *17*, 155–168.
- Kench, P. S., and R. W. Brander (2006), Wave processes on coral reef flats: Implications for reef geomorphology using Australian case studies, *J. Coastal Res.*, *22*, 209–223.
- Kench, P. S., and R. F. McLean (2004), Hydrodynamics and sediment flux of hoes in an Indian Ocean atoll, *Earth Surf. Processes Landforms*, *29*, 933–953.
- Kraines, S. B., T. Yanagi, M. Isobe, and H. Komiyama (1998), Wind-wave driven circulation on the coral reef at Bora Bay, Miyako Island, *Coral Reefs*, *17*, 133–143.
- Kraines, S. B., A. Suzuki, T. Yanagi, M. Isobe, X. Guo, and H. Komiyama (1999), Rapid water exchange between the lagoon and the open ocean at Majuro Atoll due to wind, waves and tide, *J. Geophys. Res.*, *104*(C7), 15,635–15,653.
- Kraines, S. B., M. Isobe, and H. Komiyama (2001), Seasonal variations in the exchange of water and water-borne particles at Majuro Atoll, the Republic of the Marshall Islands, *Coral Reefs*, *20*, 330–340.
- Lee, T. T., and K. P. Black (1978), The energy spectra of surf waves on a coral reef, in *Proceedings 16th International Conference on Coastal Engineering*, pp. 588–608, ASCE, Hamburg.
- Longuet-Higgins, M. S., and R. W. Stewart (1964), Radiation stresses in water waves: A physical discussion with applications, *Deep-Sea Res.*, *11*, 529–562.
- Lugo-Fernández, A., M. L. Hernández-Ávila, and H. H. Roberts (1994), Wave-energy distribution and hurricane effects on Margarita Reef, southwestern Puerto Rico, *Coral Reefs*, *13*, 21–32.
- Lugo-Fernández, A., H. H. Roberts, and W. J. J. Wiseman (1998a), Tide effects on wave attenuation and wave set-up on a Caribbean Coral Reef, *Est. Coastal Shelf Sci.*, *47*, 385–393.
- Lugo-Fernández, A., H. H. Roberts, W. J. Wiseman, and B. L. Carter (1998b), Water level and currents of tidal and infragravity periods at Tague Reef, St Croix (USVI), *Coral Reefs*, *17*, 343–349.
- Lugo-Fernández, A., H. H. Roberts, and W. J. Wiseman (2004), Currents, water levels, and mass transport over a modern Caribbean coral reef: Tague Reef, St. Croix, USVI, *Cont. Shelf Res.*, *24*, 1989–2009.
- Massel, S. R. (1996), On the largest wave height in water of constant depth, *Ocean Eng.*, *23*, 553–573.
- Massel, S. R., and R. M. Brinkman (1999), Measurement and modelling of wave propagation and breaking at steep coral reefs, in *Recent Advances in Marine Science and Technology '98*, edited by N. K. Saxena, pp. 27–36.
- Massel, S. R., and R. M. Brinkman (2001), Wave-induced set-up and flow over shoals and coral reefs: Part 1. A simplified bottom geometry case, *Oceanologia*, *43*, 373–388.
- Massel, S. R., and M. R. Gourlay (2000), On the modelling of wave breaking and set-up on coral reefs, *Coastal Eng.*, *39*, 1–27.
- Munk, W. H., and M. C. Sargent (1948), Adjustment of Bikini Atoll to ocean waves, *Trans. AGU*, *29*, 855–860.
- Nelson, R. C. (1994), Depth limited design wave heights in very flat regions, *Coastal Eng.*, *23*, 43–59.
- Nelson, R. C., and E. J. Leslie (1986), Breaker height attenuation over platform coral reefs, in *Research Report No. 12*, Univ. College, ADFA, Univ. of New South Wales, Canberra.
- Nielsen, P. (1999), Simple equipment for coastal engineering research and teaching, in *Proc. 5th COPE-DEC 99*, p. 1029–1037, Cape Town 1.
- Nielsen, P., R. W. Brander, and M. G. Hughes (2001), Rip currents: observations of hydraulic gradients, friction factors and wave pump efficiency, in *Coastal Dynamics '01*, pp. 784–796, ASCE, Lund, Sweden.
- Roberts, H. H. (1974), Variability of reefs with regard to changes in wave power around an island, in *Proc. 2nd Int. Coral Reef Symp.*, pp. 497–512.
- Roberts, H. H., and M. Suhayda (1983), Wave current interactions on a shallow reef (Nicaragua), *Coral Reefs*, *1*, 209–214.
- Roberts, H. H., S. P. Murray, and J. N. Suhayda (1977), Physical processes in a fore-reef shelf environment, in *Proc. 3rd Int. Coral Reef Symp.*, pp. 507–515, Miami.
- Roberts, H. H., P. A. Wilson, and A. Lugo-Fernández (1992), Biologic and geologic responses to physical processes: Examples from modern reef systems of the Caribbean-Atlantic region, *Cont. Shelf Res.*, *12*, 809–834.
- Seelig, W. N. (1983), Laboratory study of reef-lagoon system hydraulics, *J. Waterw. Port Coastal Ocean Eng.*, *109*, 380–391.
- Stoddart, D. R. (1969), Ecology and morphology of recent coral reefs, *Biol. Rev. Cambridge Philos. Soc.*, *44*, 433–498.
- Storlazzi, C. D., J. B. Logan, and M. E. Field (2003), Quantitative morphology of a fringing reef tract from high-resolution laser bathymetry: Southern Molokai, Hawaii, *Geol. Soc. Am. Bull.*, *115*(11), 1344–1355.
- Storlazzi, C. D., E. K. Brown, M. E. Field, K. Rodgers, and P. L. Jokiel (2005), A model for wave control on coral breakage and species distribution in the Hawaiian Islands, *Coral Reefs*, *24*, 43–55.
- Storr, J. F. (1964), Ecology and oceanography of the coral-reef tract, Abaco Island, Bahamas, *Geol. Soc. Am. Spec. Pap.*, *79*, 1–98.
- Symonds, G., K. P. Black, and I. R. Young (1995), Wave-driven flow over shallow reefs, *J. Geophys. Res.*, *100*(C2), 2639–2648.
- Tait, R. J. (1972), Wave set-up on coral reefs, *J. Geophys. Res.*, *77*(12), 2207–2211.
- Tartinville, B., and J. Rancher (2000), Wave-induced flow over Mururoa Atoll reef, *J. Coastal Res.*, *16*, 776–781.
- Tsukayama, S., and E. Nakaza (2001), Wave transformations on coral reefs, in Proceedings of the 27th International Conference on Coastal Engineering, pp. 1372–1382.
- Young, I. R. (1989), Wave transformation over coral reefs, *J. Geophys. Res.*, *94*(C7), 9779–9789.
- Zhu, L., M. Li, H. Zhang, and S. Shi-Feng (2004), Wave attenuation and friction coefficient on the coral-reef flat, *China Ocean Eng.*, *18*, 129–136.

R. W. Brander, School of Biological, Earth and Environmental Sciences, University of New South Wales, Sydney 2052, Australia. (rbrander@unsw.edu.au)

O. K. Jago and P. S. Kench, School of Geography, Geology and Environmental Science, The University of Auckland, Private Bag 92019, Auckland, New Zealand. (p.kench@auckland.ac.nz)